Earth and Planetary Science Letters, 50 (1980) 139–155
Elsevier Scientific Publishing Company, Amsterdam – Printed in The Netherlands

[6]

Sm-Nd ISOTOPIC EVOLUTION OF CHONDRITES

STEIN B. JACOBSEN and G.J. WASSERBURG

The Lunatic Asylum of the Charles Arms Laboratory, Division of Geological and Planetary Sciences, California Institute of Technology, Pasadena, CA 91125 (U.S.A.)

Received February 19, 1980
Revised version received June 3, 1980

The $^{143}Nd/^{144}Nd$ and $^{147}Sm/^{144}Nd$ ratios have been measured in five chondrites and the Juvinas achondrite. The range in $^{143}Nd/^{144}Nd$ for the analyzed meteorite samples is 5.3 ϵ-units (0.511673–0.511944) normalized to $^{150}Nd/^{142}Nd = 0.2096$. This is correlated with the variation of 4.2% in $^{147}Sm/^{144}Nd$ (0.1920–0.2000). Much of this spread is due to small-scale heterogeneities in the chondrites and does not appear to reflect the large-scale volumetric averages. It is shown that none of the samples deviate more than 0.5 ϵ-units from a 4.6-AE reference isochron and define an initial $^{143}Nd/^{144}Nd$ ratio at 4.6 AE of 0.505828 ± 9. Insofar as there is a range of values of $^{147}Sm/^{144}Nd$ there is no unique way of picking solar or average chondritic values. From these data we have selected a new set of self-consistent present-day reference values for CHUR ("chondritic uniform reservoir") of $(^{143}Nd/^{144}Nd)^0_{CHUR} = 0.511836$ and $(^{147}Sm/^{144}Nd)^0_{CHUR} = 0.1967$. The new $^{147}Sm/^{144}Nd$ value is 1.6% higher than the previous value assigned to CHUR using the Juvinas data of Lugmair. This will cause a small but significant change in the CHUR evolution curve. Some terrestrial samples of Archean age show clear deviations from the new CHUR curve. If the CHUR curve is representative of undifferentiated mantle then it demonstrates that depleted sources were also tapped early in the Archean. Such a depleted layer may represent the early evolution of the source of present-day mid-ocean ridge basalts. There exists a variety of discrepancies with most earlier meteorite data which includes determination of all Nd isotopes and Sm/Nd ratios. These discrepancies require clarification in order to permit reliable interlaboratory comparisons. The new CHUR curve implies substantial changes in model ages for lunar rocks and thus also in the interpretation of early lunar chronology.

1. Introduction

The long-lived radioactive isotope ^{147}Sm ($\lambda = 6.54 \times 10^{-12}$ yr^{-1}) which decays to ^{143}Nd is an important tracer for chemical differentiation processes affecting the rare earth (REE) and other large ion lithophile (LIL) elements during planetary evolution. When the sun and planets formed from the solar nebula, large chemical fractionations occurred especially for the volatile elements between individual solid bodies in the solar system. It is, however, usually assumed that bulk planets have solar relative REE and other refractory LIL element abundances. The solar chemical data compiled by Ross and Aller [1] support the suggestion by Goldschmidt [2] that chondritic meteorites give the best clues to solar system abundances of the non-volatile elements. Knowledge of the *average* chondritic or solar values of Sm and Nd isotopes is therefore extremely important in the interpretation of Sm-Nd data and modeling of planetary evolution. The purpose of this paper is to obtain an estimate of the average solar system values for $^{147}Sm/^{144}Nd$ and $^{143}Nd/^{144}Nd$ using chondrite samples. Our ability to determine the solar values depends on whether the solar nebula was initially isotopically homogeneous for the elements of interest and whether we have samples of material which are chemically unfractionated in Sm relative to Nd. Direct measurements of the abundances of Nd and Sm in the Sun have recently been made by Maier and Whaling

Division of Geological and Planetary Sciences, Calfornia Institute of Technology, Contribution No. 3371 (336).

0012-821X/80/0000–0000/$02.25 © 1980 Elsevier Scientific Publishing Company

[3] and Saffman and Whaling [4], respectively. These studies give $\log_{10}(N_{Nd}/N_H) + 12 = 1.26 \pm 0.14$ and $\log_{10}(N_{Sm}/N_H) + 12 = 0.80 \pm 0.11$ for the Sun from which we calculate $(^{147}Sm/^{144}Nd)_{\odot} = 0.22$ (+0.16, −0.09). This value has a relatively large uncertainty. A least squares analyses of all the REE in the Sun [1] and in CII chondrites, however, suggest that $(^{147}Sm/^{144}Nd)_{\odot} = 0.209 \pm 0.013$ and is within 10% of that in CII chondrites (Nyquist, personal communication). This value can at best serve as a guide in the subsequent discussion and it appears that the most reliable estimate of the solar value of $^{147}Sm/^{144}Nd$ is from the study of chondritic meteorites. If a relatively well-defined average value can be obtained for $^{147}Sm/^{144}Nd$ in chondrites, then this may be used in turn to define the solar $^{143}Nd/^{144}Nd$ value.

In this paper we present Sm-Nd results for two carbonaceous chondrites (Murchison and Allende), three ordinary chondrites (Peace River, Guareña, and St. Severin), and one achondrite (Juvinas). Murchison is classified as a CM2 chondrite which comprises the most abundant type of carbonaceous chondrites. Allende is a CV3 chondrite and is considered the petrologically most primitive class of carbonaceous chondrites [5]. It contains inclusions of high-temperature condensates, some of which have the most primitive $^{87}Sr/^{86}Sr$ ratio so far found [6], and inclusions which are isotopically anomalous for Sm and Nd [7,8] as well as for other elements. Peace River is an L6 chondrite which is a class that constitutes the most abundant of ordinary chondrites. Guareña and St. Severin are H6 and LL6 chondrites, respectively, which have been extensively studied for Rb-Sr, U-Th-Pb, and I-Pu-Xe systematics because of their high content of whitlockite [9–13]. Finally, Juvinas is a basaltic achondrite which has a Sm/Nd ratio close to the average chondritic value and apparently crystallized early in the history of a basaltic achondrite parent body [14]. Preliminary reports of these results were made at the Eleventh Lunar and Planetary Science Conference [15] and in S.B.J.'s Ph.D. thesis [16].

The first survey of REE in chondrites [17–19] by neutron activation analysis demonstrated a reasonable degree of consistency in relative abundances of REE with an accuracy of about 10%. Later the isotope dilution technique was applied to REE in chondrites [20–26] with the precision for individual REE considered to be 1–2%. Both techniques are subject to uncertainties in the absolute concentration in reference standards [20]. The concentration levels of REE in chondrites are fairly low (~0.6 ppm Nd) and no measurements exist on chondrites for both $^{143}Nd/^{144}Nd$ and $^{147}Sm/^{144}Nd$ except for the data of Notsu and Mabuchi [27] which have large analytical uncertainties (15 ϵ-units in $^{143}Nd/^{144}Nd$ and ~4% in $^{147}Sm/^{144}Nd$). A 1% error in the Sm/Nd ratio adds an error of 1.1 ϵ-units to the $^{143}Nd/^{144}Nd$ ratio over 4.5 AE (1 ϵ-unit $\equiv$ 0.01%). Therefore, it is necessary to measure both the $^{147}Sm/^{144}Nd$ and $^{143}Nd/^{144}Nd$ ratios with high precision to establish a $^{143}Nd/^{144}Nd$ evolution curve. We are currently able to routinely measure the $^{147}Sm/^{144}Nd$ ratio with an accuracy of 0.05% and the error added to a $^{143}Nd/^{144}Nd$ evolution curve from the measurement of the Sm/Nd ratio is therefore insignificant (i.e., it is 0.06 ϵ-units). The first substantial meteorite measurements were made by Lugmair et al. [28], who chose a basaltic achondrite (Juvinas) which had a $^{147}Sm/^{144}Nd$ isotope ratio close to the average chondritic value. Lugmair et al. [29] used the Juvinas values as an approximation to chondritic Sm-Nd evolution which is justified if the source of Juvinas on the basaltic achondrite parent body (BACH) did not have a long prehistory as is suggested by Rb-Sr and Sm-Nd internal isochrons for Juvinas [30,14].

2. Sm-Nd systematics of chondrites

The refractory lithophile elements Si, Mg, and Cr show a factor of two fractionation relative to Al between individual chondrite classes. This is most likely due to fractional condensation [31]. The extent to which condensation processes have fractionated Sm relative to Nd in individual chondrite classes relative to each other and the average solar system is not precisely known. Boynton [32] has modelled the condensation of REE and showed that large fractionations may occur among the heavy REE in the solar nebula at high temperature (>1600°K) while the light REE (La, Pr, Nd, Sm) are expected to show only small relative fractionations during condensation. The elements Ce, Eu, and Yb have variable valence states and may be expected to show large abundance anomalies. This is consistent with REE patterns

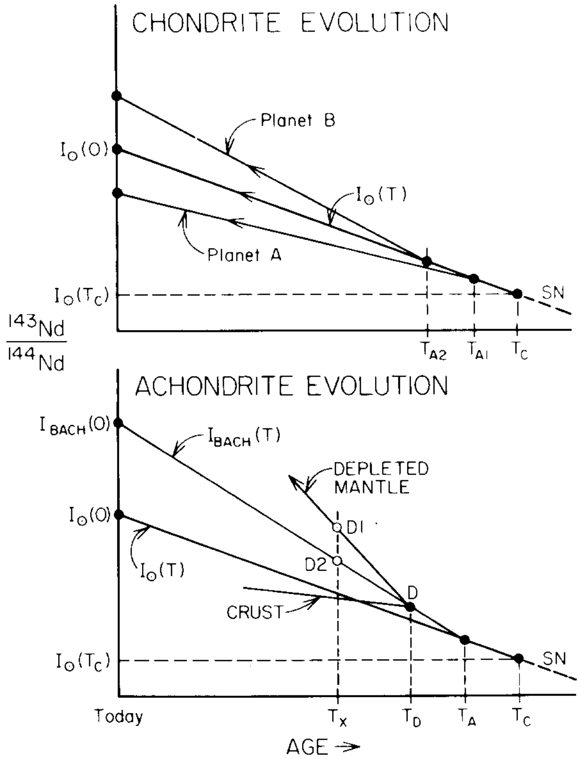

Fig. 1. Schematic representation of the evolution of $^{143}Nd/^{144}Nd$ with time for chondritic and achondritic parent bodies. Solid objects started to condense from the solar nebula (*SN*) at time T_C and accreted to parent bodies at time T_A. Subsequent to T_A a part of the parent bodies of achondrites may have differentiated at T_D into crust and depleted mantle. At times T_X subsequent to T_D, melts may be tapped from both depleted mantle (*D1*) and from previously undifferentiated material (*D2*).

obtained on high-temperature condensates in CM and CV meteorites [26,33].

We now wish to consider some simple evolutionary histories of planetary objects that condensed and accreted from the solar nebula and are assumed to have a well-defined average Sm/Nd ratio. The time evolution is shown schematically in Fig. 1. At T_C (about 4.6 AE ago) solid objects began condensing from the solar nebula (*SN*), from which the planets and meteorites are ultimately derived. The rate of growth of $^{143}Nd/^{144}Nd$ in these planetary objects may be different from the solar value due to variations in the relative chemical abundances of Sm and Nd during condensation and accretion. If a reservoir j is a closed system, then the evolution of $^{143}Nd/^{144}Nd$ as a function of time T is defined as $I_j^{Nd}(T)$ with $I_j^{Nd}(0)$ being the present-day value. The value of $^{143}Nd/^{144}Nd$ at any time in the past in reservoir j is:

$$I_j^{Nd}(T) = I_j^{Nd}(0) - \left(\frac{^{147}Sm}{^{144}Nd}\right)_j^0 [\exp(\lambda T) - 1] \qquad (1)$$

where $(^{147}Sm/^{144}Nd)_j^0$ is the value in j today. Most meteorites come from small planetary objects and have ages within ~0.1 AE of the time of condensation and accretion from the solar nebula and provide important clues to the Sm/Nd isotopic evolution of the solar system. The objects of interest include meteorites which formed by melting processes on parent planets such as achondrites and the more primitive chondrites which appear to be aggregates of high- and low-temperature condensates from the solar nebula.

The evolution of chondritic meteorite parent bodies is shown schematically in Fig. 1; planet A accretes at time T_{A1} with a Sm/Nd ratio lower than the solar value and planet B accretes at time T_{A2} with Sm/Nd higher than the solar value. If $T_{A1} = T_{A2}$ then the initial $^{143}Nd/^{144}Nd$ values of the two planetary bodies would be equal according to this model. Chondritic planetary bodies may be heterogeneous such that different chondritic meteorites from the same planet could have different Sm/Nd ratios. DePaolo and Wasserburg [34] introduced the acronym CHUR ("chondritic uniform reservoir") for a bulk planet with $^{147}Sm/^{144}Nd$ *ratio* and $^{143}Nd/^{144}Nd$ isotopic ratio the same as in *average* chondrites.

In contrast to chondrites, achondrites are fragments of planetary crusts that began to form by partial melting at the time of early chemical differentiation of a parent body (T_D) subsequent to condensation and accretion and will show an evolution as is illustrated schematically in Fig. 1. Magmatic rocks formed subsequent to T_D at T_X may be derived from light-REE-depleted mantle. There could be a 0.1 AE time difference between planet formation and melting, which for a source region having a $^{147}Sm/^{144}Nd$ which is 20% higher than the chondritic value would give a 1.0 ϵ-unit difference from the solar value of the $^{143}Nd/^{144}Nd$ growth curve at the time of melting.

If there were reservoirs that were isolated with negligible amounts of the radioactive parent ^{147}Sm near T_C (Sm/Nd $\approx$ 0), samples of such materials would record today the $^{143}Nd/^{144}Nd$ value at or near the time of condensation. Because of the limited range in Sm/Nd for minerals in meteorites, it has so far proven difficult to measure T_C and $I_{\odot}^{Nd}(T_C)$ precisely. The evolution of $^{143}Nd/^{144}Nd$ in the solar nebula changes by 2.6 ϵ-units in 100 m.y. This relatively slow rate of evolution and the lack of large fractionations in Sm relative to Nd makes the Sm-Nd system a rather insensitive chronometer for the relative times of condensation of solid objects from the solar nebula. Thus the lowest $^{143}Nd/^{144}Nd$ ratio ever measured is 0.508880 ± 22 [35] and is still 59 ϵ-units higher than the initial solar value.

It is instructive to compare the Sm-Nd system with the solar evolution of the Rb-Sr and U-Th-Pb systems. There is such major chemical fractionation in the U-Th-Pb and Rb-Sr systems that ancient materials exist today which contain Pb and Sr that are very close to the initial solar system values. For example, troilite inclusions in iron meteorites give $^{238}U/^{204}Pb$ = 0.001 and have measured $^{206}Pb/^{204}Pb$ isotope ratios which are essentially within error of the primordial values [36,37]. For the U-Pb system the radiogenic daughter Pb is a volatile element and there is a low present-day solar value of $(^{238}U/^{204}Pb)_{\odot} \approx 0.2$ [1, 38–40]. We calculate a change in $^{207}Pb/^{204}Pb$ in the solar nebula at 4.6 AE of 13ϵ-units in 100 m.y. and a change in $^{206}Pb/^{204}Pb$ of 7 ϵ-units in 100 m.y. In contrast high-temperature condensates, earth, moon, and eucrites have bulk $^{238}U/^{204}Pb$ in the range from ~10 to 250 and thus have highly radiogenic leads. Initial Pb values for meteorites can at best be measured to ±3 ϵ-units and are therefore not very sensitive to the times of condensation from the solar nebula, while the highly radiogenic leads in volatile poor objects are good chronometers for early solar system processes. For Rb-Sr, achondrites, some ancient lunar samples, and high-temperature condensates in Allende have $^{87}Rb/^{86}Sr$ in the range 0.001–0.003 [6,41–45], so their initial $^{87}Sr/^{86}Sr$ can be almost directly obtained essentially independent of their precise age. The radioactive parent ^{87}Rb is a volatile element and the Sun has a high $(^{87}Rb/^{86}Sr)_{\odot} = 1.4$ [46] and consequently a highly radiogenic $^{87}Sr/^{86}Sr$ ratio. The $^{87}Sr/^{86}Sr$ ratio in the solar nebula thus changes by 28 ϵ-units in 100 m.y. and is, therefore, a very sensitive chronometer for the relative times of condensation of solid objects from the solar nebula.

3. Samples

The Allende sample (A6) is a split from a 30-gram total meteorite sample prepared by Gray et al. [6]. For Guareña a 193-gram total meteorite sample was powdered (<75 μm) from which the metallic phase was removed. The total meteorite concentrations of Sm and Nd in Table 1 have been corrected for the removed metal. St. Severin is known to consist of light and dark colored areas [10,13]. Two 3-gram pieces from light and dark colored areas respectively of sample H2402b were used for this work. The Peace River sample is a split from a 200-gram total meteorite sample prepared by Gray et al. [6]. The Juvinas sample (no. 40, piece A) is a 1.2-gram piece of the total meteorite. For Murchison sample Me2642, three different pieces (no. 1, no. 2, and no. 3) were used. Pieces no. 1 and no. 2 weighed several grams and were powdered before dissolution. Piece no. 3 weighed 1.1 grams and was dissolved without first being powdered. To minimize effects from sample heterogeneity the amount of material dissolved in each experiment is relatively large and is given in Table 1.

4. Analytical procedures

The samples were dissolved in HF and $HClO_4$. The samples Murchison no. 1, Allende, and Peace River were each split into three aliquots (ALIQ-1, 2, 3) after dissolution. ALIQ-1 and 3 were totally spiked while ALIQ-2 was unspiked with Sm and Nd tracers. All other samples were totally spiked with Sm and Nd tracers after dissolution. Separation of Sm and Nd follows the procedure described for Gd by Eugster et al. [47] with the slight modifications reported by DePaolo and Wasserburg [34]. The total procedural blank for Nd is 25 pg or less and $^{147}Sm/^{144}Nd$ = 0.14 for the blank. Typically aliquots containing ~100 mg sample were passed through the ion exchange columns and individual separations from meteorites thus yielded 60 ng of Nd or more so the blanks are insignificant. Nd and Sm isotopic compositions were measured on the Lunatic I and III mass spectrometers [48] as NdO^+ and Sm^+, respectively, following the procedures described in detail by DePaolo and Wasserburg [34], Papanastassiou et al.

[49], and DePaolo [50]. For NdO^+ the ion beam intensity at mass 160 ($^{144}Nd^{16}O$) was 10^{-11} A and ion beam intensity ratios were calculated relative to mass 160. Interference from SmO^+ is then corrected from measurement of mass 170 ($^{154}Sm^{16}O$) which is typically 5×10^{-16} A. Interferences from other species were always insignificant. Oxygen corrections were then made using $^{18}O/^{16}O = 0.002045$ and $^{17}O/^{16}O = 0.0003708$ [51]. Mass discrimination corrections were then made with a linear law using $^{150}Nd/^{142}Nd = 0.2096$ for unspiked runs and $^{146}Nd/^{142}Nd = 0.636151$ for spiked runs. Concentrations were determined using ^{150}Nd and ^{147}Sm tracers. Extensive calibrations of tracers with normal solutions made up from ultrapure Nd and Sm metals from Ames Laboratory, Iowa, demonstrate that we can routinely measure the $^{147}Sm/^{144}Nd$ ratio to 0.05%. Details of these calibrations will be discussed elsewhere. The grand mean values of terrestrial normals for nonradiogenic Nd isotopes (Table 1) used are those by McCulloch and Wasserburg [7] which are updated from those of DePaolo and Wasserburg [52] and Papanastassiou et al. [49]. The grand mean values of terrestrial normals for Sm isotopes (Table 1) used are those of Russ [53] which are updated from those of Russ et al. [54]. These updated ratios for both Nd and Sm show no change with time and the acquisition of new data and are essentially indistinguishable from the original values of DePaolo and Wasserburg [52] and Russ et al. [54]. Insofar as all non-radiogenic isotopes agree from run to run and meteorite data are also in agreement, this means that the choice of normalization isotopes cannot account for discrepancies for data taken in this laboratory with those of other laboratories. However, if some error is made in measurement of the normalization isotopes, it certainly will affect the comparison of data from different laboratories.

5. Results

The Sm-Nd results are given in Tables 1 and 2 and Fig. 2. We first note that all non-radiogenic isotope ratios are within error of the grand mean of our terrestrial normals and lunar samples measured in this laboratory [49]. There are thus no widespread isotopic anomalies in Nd for bulk chondrite samples to within

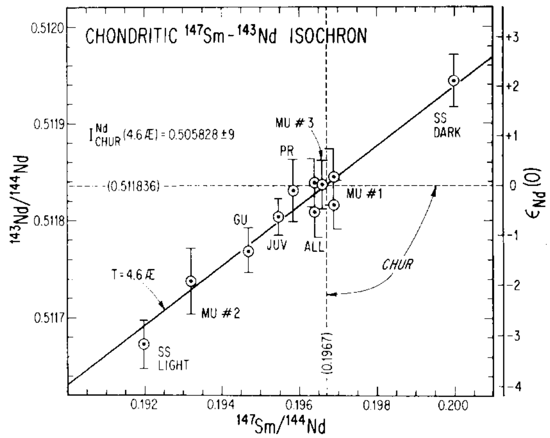

Fig. 2. Sm-Nd evolution diagram for chondrite samples and Juvinas. A reference line with a slope of 4.6 AE is shown. The dashed lines represent the new values selected for average chondrites (CHUR).

±0.5 ϵ-units. These results show the self-consistency of the data as indicated above. For Sm we routinely measured all isotopes except ^{150}Sm and ^{144}Sm and confirmed that $^{149}Sm/^{154}Sm$ are within error (±1.0 ϵ-units) the same as the terrestrial values. The absence of any neutron capture effects on ^{149}Sm is consistent with the short exposure ages of these meteorites [47, 54]. This justifies the use of $^{143}Nd/^{144}Nd$ and $^{147}Sm/^{144}Nd$ isotope ratios calculated from spiked runs using the grand mean values of terrestrial normals for Sm and Nd isotopic compositions.

The data in Table 1 are shown on a Sm-Nd evolution diagram relative to a reference line with a slope corresponding to an age of 4.60 AE. A variety of chondrites and the achondrite Juvinas lie within ±0.5 ϵ-units of the reference line shown. This conclusion is insensitive to the particular choice of age in a plausible neighborhood of 4.6 AE. The present-day range in these chondrite samples is 5.3 ϵ-units in $^{143}Nd/^{144}Nd$ and 4.2% in $^{147}Sm/^{144}Nd$. If all chondrites are isochronous and from an isotopically uniform source, they should today lie on a line with a slope of 4.6 AE in a Sm-Nd evolution diagram. The values of $^{143}Nd/^{144}Nd$ corrected back to 4.6 AE ago are also given in Table 1. The total range is only 0.9 ϵ-units and the average value of $^{143}Nd/^{144}Nd$ at 4.6 AE is 0.505828 ± 9.

TABLE 1

Sm–Nd isotopic results [a]

Sample	Weight [b] (g)	Nd(ppm)	Sm(ppm)	$^{147}Sm/^{144}Nd$	$^{143}Nd/^{144}Nd$	I^{Nd}(4.6 AE)
I. Murchison (CM2)						
#1-ALIQ-1	0.51	0.63495	0.20671	0.19693 [a]		–
#1-ALIQ-2		–	–	–	0.511845 ± 29 [d]	0.505831 ± 32
#1-ALIQ-3		0.63506	0.20672	0.19691	0.511816 ± 25 [c]	0.505802 ± 28
#2	0.44	0.67034	0.21409	0.19320	0.511738 ± 34 [c]	0.505834 ± 37
#3	1.12	0.64312	0.20903	0.19661	0.511837 ± 25 [c]	0.505832 ± 28
II. Allende (CV3)						
ALIQ-1	2.61	0.86957	0.28230	0.19639 [a]	–	–
ALIQ-2		–	–	–	0.511809 ± 26 [d]	0.505811 ± 29
ALIQ-2		–	–	–	0.511839 ± 25 [d]	0.505841 ± 28
III. Guareña (H6)						
	2.52	0.90208	0.29031	0.19468	0.511769 ± 24 [c]	0.505823 ± 27
IV. Peace River (L6)						
ALIQ-1	2.97	0.69854	0.22615	0.19584 [a]	–	–
ALIQ-2		–	–	–	0.511831 ± 32 [d]	0.505850 ± 35
V. St. Severin (LL6)						
Light	2.86	1.38562	0.43972	0.19197	0.511673 ± 25 [c]	0.505810 ± 28
Dark	2.93	0.55993	0.18513	0.20001	0.511944 ± 27 [c]	0.505836 ± 30
VI. Juvinas						
ALIQ-1	1.24	5.5245	1.7848	0.19543	0.511804 ± 19 [c]	0.505835 ± 22

[a] Reported errors are 2 of the mean.
[b] Weight of dissolved sample.
[c] Sample spiked with ^{150}Nd and ^{147} Sm tracers. Data normalized to $^{146}Nd/^{142}Nd = 0.636151$ and $^{148}Sm/^{154}Sm = 0.49419$. Concentrations calculated using $^{142}Nd/^{144}Nd = 1.138266$, $^{145}Nd/^{144}Nd = 0.348968$, $^{146}Nd/^{144}Nd = 0.724109$, $^{148}Nd/^{144}Nd = 0.243079$, $^{150}Nd/^{144}Nd = 0.238581$ [7] and an atomic weight of 144.24 for Nd. For Sm we used an atomic weight of 150.35 and the isotopic composition reported by Russ et al. [54] and Russ [53]; $^{144}Sm/^{154}Sm = 0.13516$, $^{147}Sm/^{154}Sm = 0.65918$, $^{149}Sm/^{154}Sm = 0.60750$, $^{150}Sm/^{154}Sm = 0.32440$, $^{152}Sm/^{154}Sm = 1.17537$.
[d] Unspiked samples normalized to $^{150}Nd/^{142}Nd = 0.2096$.

Insofar as there is variation in the Sm/Nd ratio between chondrite samples, there is no unique way of picking a set of values for $^{143}Nd/^{144}Nd$ and $^{147}Sm/^{144}Nd$ as representing the true solar ratio. The best we can do from the data is to pick a single set of reference values for $^{143}Nd/^{144}Nd$ and $^{147}Sm/^{144}Nd$ today that are consistent with the data array in Fig. 2. The approach used here will be to define the best present-day "solar" reference values rather than the initial values at T_C. This follows the approach adopted by DePaolo and Wasserburg [34] who referred evolution curves to determinations of the modern values rather than the derived initial values. For simplicity the approach we have chosen is to take the modern value for $^{143}Nd/^{144}Nd = 0.511836$, which is the currently used value for CHUR, as this will cause the least shift in the data representations and is fully consistent with the chondritic values. The corresponding $^{147}Sm/^{144}Nd$ ratio on the reference isochron is 0.1967 and lies close to the data for Allende and two of the Murchison samples. Including the new data in Table 1 there are now 64 determinations of $^{147}Sm/^{144}Nd$ in bulk chondrite samples by isotope dilution. All these data are shown in a histogram in Fig. 3. As indicated, the value we have chosen lies close to the peak of the histogram. The previously published data are not accurate to better than about ±2% and most of the data actually are within 2% of the average value chosen for chondrites. However, clear exceptions occur especially for the E chondrites

TABLE 2

Results for non-radiogenic Nd isotopes [a]

Sample	ϵ_{142}	ϵ_{145}	ϵ_{146}	ϵ_{148}
I. Murchison				
#1-ALIQ-2	−0.4 ± 0.4	+0.6 ± 0.7	+0.5 ± 0.7	−0.7 ± 1.1
#1-ALIQ-3	−0.5 ± 0.4	−0.8 ± 0.6	–	–
#2	−0.2 ± 0.5	+0.5 ± 0.9	–	−0.4 ± 1.6
#3	−0.3 ± 0.4	+0.3 ± 0.8	–	−0.1 ± 0.9
II. Allende				
ALIQ-2	0.0 ± 0.4	+0.4 ± 0.5	0.0 ± 0.5	+0.5 ± 1.0
ALIQ-2	+0.1 ± 0.6	+0.1 ± 0.5	0.0 ± 0.5	+0.7 ± 0.6
III. Guareña				
	+0.3 ± 0.4	−0.9 ± 0.6	–	−0.3 ± 0.9
IV. Peace River				
ALIQ-2	+0.4 ± 0.4	+0.1 ± 0.7	−0.6 ± 0.7	−0.1 ± 1.0
V. St. Severin				
Light	−0.2 ± 0.4	+0.3 ± 0.5	–	+0.2 ± 1.1
Dark	−0.2 ± 0.3	+0.2 ± 0.4	–	+0.1 ± 0.8
VI. Juvinas				
ALIQ-1	−0.1 ± 0.4	+0.1 ± 0.5	–	+0.1 ± 0.8

[a] ϵ-values are given as deviations in parts in 10^4 relative to the grand mean of terrestrial normals given in Table 1. Reported errors are 2σ of the mean.

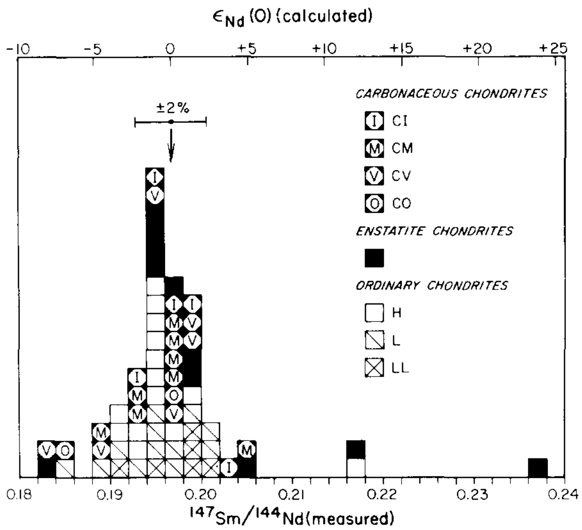

Fig. 3. Histogram showing all available $^{147}Sm/^{144}Nd$ ratios (N = 64) for chondritic meteorites determined by isotope dilution methods. The ratios from previously published REE studies on chondrites [20–27] are probably accurate to ~2%. Chondritic meteorites show a large range in $^{147}Sm/^{144}Nd$, with most of the data in the range from 0.188 to 0.206. The value selected for average chondrites of 0.1967 is close to the peak of the histogram and is shown by the arrow. The $\epsilon_{Nd}(0)$ value calculated assuming T_C = 4.6 AE is shown on the top of the figure. It is evident from these data that a total rock isochron for chondrites may be determined.

which show a variation in $^{147}Sm/^{144}Nd$ from 0.183 to 0.236. However, the averages of each class of chondrites show a smaller range in $^{147}Sm/^{144}Nd$. The averages of C, E, H, L, and LL chondrites are 0.195, 0.202, 0.196, 0.195, and 0.197, respectively. These values are all within error of each other and identical to the much less precisely known solar value of $(^{147}Sm/^{144}Nd)_{\odot} = 0.2$. It is clear that the average values for each class appear to be well defined compared to the values for individual samples. We conclude from the convergence of the values that the parent planets of the individual chondrite classes have a small range in $^{147}Sm/^{144}Nd$. In chondrites there is, however, on a centimeter scale much larger heterogeneity in the $^{147}Sm/^{144}Nd$ ratio. A special effort was made to investigate this heterogeneity in St. Severin. Jones and Burnett [13] have shown that

St. Severin consists of ~30% light-colored material and 70% dark-colored material. We obtained a 4% difference in the $^{147}Sm/^{144}Nd$ between samples of light- and dark-colored material. We calculate a "total rock value" for St. Severin of $^{147}Sm/^{144}Nd = 0.1959$ from the data in Table 1 using the proportions determined by Jones and Burnett [13]. This value is much closer to the average value we have chosen for CHUR than the samples we measured of the light and the dark material.

The chemical abundances in CI1 carbonaceous chondrites have a special significance since they compare very closely with the abundances of the condensable elements which can be reliably measured from studied of the photospheric spectrum of the Sun. However, they are not pristine samples of solar system condensate as they show the highest degree of low-temperature alteration among the carbonaceous chondrites [5]. The average $^{147}Sm/^{144}Nd$ of CI1 chondrites is 0.197 on the basis of four measurements of Orgueil and one of Ivuna [24,25] and is close to that of other chondrite classes. The individual samples, however, do show a 6% range in $^{147}Sm/^{144}Nd$ (0.192–0.204) so it appears that the CI1 chondrites show the same small-scale heterogeneity as other chondrites and a unique value cannot easily be obtained from these objects.

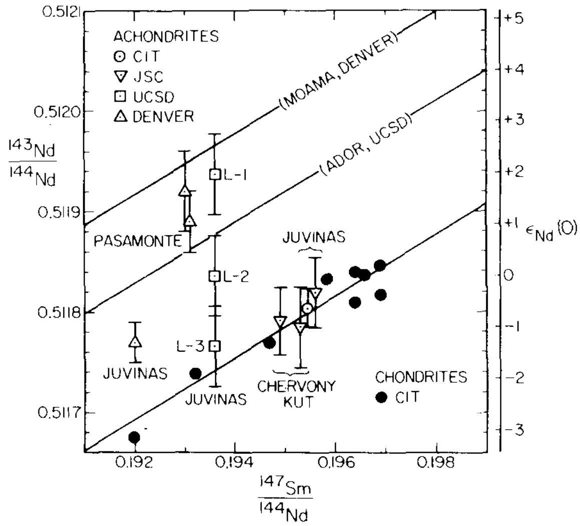

Fig. 4. Sm-Nd evolution diagram comparing new chondrite data (black dots) and the Juvinas value with previously published data for achondrites. The points labelled *L1*, *L2*, and *L3* represent three successive versions of the Juvinas total rock value by Lugmair et al. [28,29,58] and Lugmair and Carlson [59]. Note the discrepancies between different laboratories.

6. Comparison with previously published data

Previously published data on basaltic achondrites that fall in the neighborhood of our chondrite data are shown (Fig. 4) together with our new data on chondrites and Juvinas. The isochrons of ADOR [55] and Moama [56] are also shown, although all the data for these meteorites plot far outside the diagram. Let us first compare the Juvinas total rock data from various laboratories. The first report was by Notsu et al. [57] who presented some rather imprecise data. The first high-precision data on Juvinas were published by Lugmair [14] and Lugmair et al. [28], and they reported two total rock values together with data for pyroxene and plagioclase. A spread of 42 ϵ-units in $^{143}Nd/^{144}Nd$ and 42% in Sm/Nd was given for the minerals. For some reason they did not report the abundances of all the Nd isotopes. A selected total rock value was used by Lugmair et al. [29] to approximate chondritic evolution (L1) and is about 3.8 ϵ-units above our 4.6-AE reference line. A revised value (L2) which has never been fully documented was reported by Lugmair et al. [58] and is 1.9 ϵ-units above our reference line. Lugmair and Carlson [59] reported a 1.4 ϵ-unit reduction in the measured $^{143}Nd/^{144}Nd$ ratio for their laboratory standard. They chose, however, to apply a correction factor to their new data such that they were compatible with their previously published data. Their currently measured Juvinas value (L3) without this correction would thus be 1.4 ϵ-units lower and as shown in Fig. 4 this value is within error of our 4.6-AE reference line. Comparison of values on a UCSD standard reported by Nyquist et al. [45], however, suggests that we should compare our $^{143}Nd/^{144}Nd$ ratios with the L2 value of Lugmair et al. [58]. The value obtained by Nakamura et al. [60] for Juvinas plot distinctly above the reference line. Their value is the same as L3 for $^{143}Nd/^{144}Nd$ but has a lower Sm/Nd ratio. Recently Nyquist et al. [45] published data on Juvinas which agree with the measured (not corrected) $^{143}Nd/^{144}Nd$ L3 ratio by Lugmair and the value by Nakamura et al. [60] but with a significantly higher $^{147}Sm/^{144}Nd$ ratio. Data on Juvinas by Nyquist et al. [45] and the data obtained independently by us agree to within 0.1% for $^{147}Sm/^{144}Nd$ and 0.3 ϵ-units for $^{143}Nd/^{144}Nd$. It would appear that the data of Nakamura et al. [60] and the revised data (L3) of Lugmair and Carlson [59] are consistent with the $^{143}Nd/^{144}Nd$ obtained by Nyquist et al. [45] and ourselves, but their $^{147}Sm/^{144}Nd$ ratios are significantly lower and suggest an error in tracer calibrations or in isotopic abundances by these workers. The situation may, however, be more complex than a simple error in tracer calibration. Fig. 5 of Nyquist et al. [45] shows the JSC and UCSD data to agree except for eucrites. The data for Pasamonte [61], Moama [56], and ADOR [55] also lie significantly above our reference line (Fig. 4). Comparison between the results of Nyquist et al. [45] and our data on achondrites seems to be confirmatory. We note, however, that Nyquist et al. [45] obtained metals (cation impurities <100 ppm) for tracer calibration from the same source that we have been using (Ames Laboratory, Iowa), so both laboratories would have the same systematic errors in tracer calibrations if there are substantial anion impurities in the metal (O, C, N, Cl). It should be noted that the normal values measured for $^{142}Nd/^{144}Nd$, $^{150}Nd/^{144}Nd$ reported by Nyquist et al. [45] differ significantly from our values while the remaining isotope ratios show good agreement. Thus the results from these two laboratories are not as consistent as might be believed on superficial inspection. It is apparent that the actual cause of all the above discrepancies must be resolved before any progress can be made in interlaboratory comparisons. Using two different mass spectrometers in this laboratory for hundreds of Nd analyses, we observe no shift in the values of the non-radiogenic Nd isotopes over the past five years. In the same period, three different Nd and three different Sm tracer calibrations show no discrepancies exceeding 0.1%. We measure Nd as NdO^+ so if the oxygen isotope composition used to reduce the data is incorrect then our data will be systematically biased [49]. This bias would only become apparent when comparing our data to that of others, such as Nyquist et al. [45] who measured Nd^+. Unless the oxygen correction procedure is subject to serious problems, we consider the measurements presented here to be reliable and to provide reasonable and consistent values for the chondritic $^{143}Nd/^{144}Nd$ and $^{147}Sm/^{144}Nd$ today. These values may be used as the basis for calculating the CHUR curve. It is important to recognize that if a mass spectrometer system is truly linear, if the mass resolution is sufficient, and if isotopic mass fractionation is small, then all of the isotopic ratios should be congruent by a mass fractionation correction and the results will be independent of the isotopic pair used for normalization inside of intrinsic precision. It follows that the choice of normalization cannot be an explanation of the isotopic discrepancies in a simple way for well designed systems.

7. Initial values

The deviations in ϵ-units for all the samples measured from the new CHUR reference curve are shown in Fig. 5 as a function of time from today to 5 AE ago. Two black boxes (*A* and *B*) are shown in Fig. 5 at 4.6 AE and 3 AE, respectively, representing variation in time of ±0.1 AE and variation in $^{143}Nd/^{144}Nd$ of ±0.5 ϵ-units. As shown in the neighborhood of 4.6 AE the $^{143}Nd/^{144}Nd$ evolution curves for all samples measured converges to within 0.5 ϵ-units of the new CHUR reference curve. This is also true at 3 AE ago except for the dark and light fractions of St. Severin

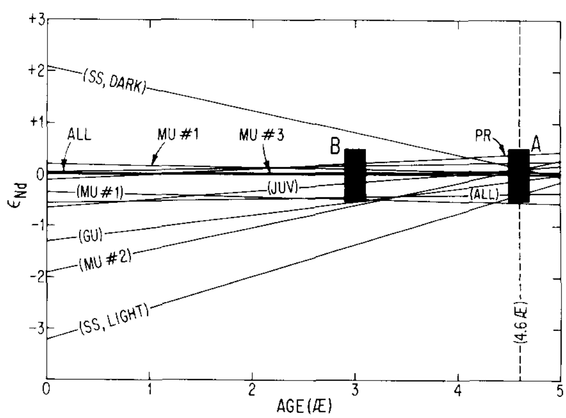

Fig. 5. ϵ_{Nd} evolution curves for chondrite and Juvinas data reported in this paper. The black boxes *A* and *B* represent ±0.5 ϵ-unit and ±100 m.y. at 4.6 AE and 3 AE ago, respectively.

which have a large spread in the Sm/Nd ratio. A calculated "total meteorite" value for St. Severin would also be within 0.5 ϵ-units of the CHUR curve at 3 AE ago. Thus the average chondritic (and presumably solar) evolution curve is defined to within ±0.5 ϵ-units of the selected CHUR reference curve in the time from 3 AE to 4.6 AE ago. This conclusion is *independent* of the detailed choice of present-day reference values for CHUR. For more recent times the deviations from the CHUR reference curve are somewhat larger, being up to 2 ϵ-units for total meteorite data.

We note that Hamilton et al. [62] have chosen an initial state using the initial $^{143}Nd/^{144}Nd$ from ADOR and the age of ADOR together with average Sm/Nd determined from REE-studies of chondrites by Evensen et al. [25] as a reference value for the CHUR curve. This selection is inconsistent with the new CHUR curve presented here (i.e., $^{143}Nd/^{144}Nd$ is higher by ~2.5 ϵ-units for all time) due to the fact that the ADOR initial value does not plot on it.

The $^{143}Nd/^{144}Nd$ ratio in CHUR as a function of time in the neighborhood of 4.5 AE is shown in Fig. 6. Assuming that a meteorite formed from this reservoir at $T = 4.6$ AE, it should have an initial $^{143}Nd/^{144}Nd$ value of 0.505829 from the selected present-day reference values for CHUR. This value is identical to the value calculated above (0.505828 ± 9) from the direct measurements on individual meteorites. We note that $^{143}Nd/^{144}Nd$ changes by 1 ϵ-unit in 39 m.y. The time scale for condensation and chemical fractionation from the solar nebula is probably on the order of only a few million years as suggested by the presence of ^{26}Al [63,64]. If the ^{26}Al is the cause of widespread heating and differentiation of small planetary bodies, then these planets must have accreted within ~2 m.y. of the time of condensation from the solar nebula [42]. Chondrites (e.g., Allende) exist that appear to preserve direct early condensates from the solar nebula which are only partly affected by later metamorphism. A reliable value for both the solar system initial Nd value and the time may be gotten if it is possible to obtain precise ages (±10 m.y.) and initial values to ±0.3 ϵ-units on such samples with an internal mineral isochron. If large planetary objects took about 10^8 years to form as suggested by Safranov [65] from theoretical considerations, and inferred by Tera and Wasserburg [66], and Gancarz and Wasserburg [67] from observational results, then the initial $^{143}Nd/^{144}Nd$ could be about 2.5 ϵ-units higher than that from the early condensates from the solar nebula. Although the initial state is not well known, we may in principle pick any set of self-consistent initial $^{143}Nd/^{144}Nd$, age, and Sm/Nd ratio that plot on the CHUR curve as reference values to describe the CHUR evolution curve instead of the present-day values we are using. In absence of directly measured initial solar values [i.e., T_C, $I_{\odot}^{Nd}(T_C)$], it is important to pick a set of reference values which the solar system is believed to have passed through and that is prior to planetary differentiation processes. Model ages [68] may be calculated relative to such a chosen initial Nd value $[I_{\odot}^{Nd}(T_C)]$ for the solar system:

$$T_M^{Nd} = \frac{1}{\lambda} \ln \left[1 + \frac{(^{143}Nd/^{144}Nd)_{MEAS} - I_{\odot}^{Nd}(T_C)}{(^{147}Sm/^{144}Nd)_{MEAS}} \right] \quad (2)$$

and should be compared to the corresponding initial time T_C on the CHUR curve. We may pick the values shown in Fig. 6 as $T_C = 4.60$ AE and $I_{\odot}(T_C) = 0.505829$. Samples which have T_M^{Nd} close to

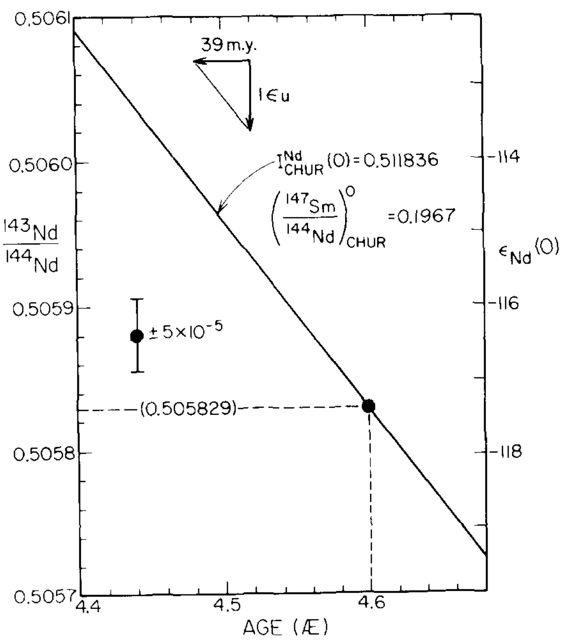

Fig. 6. The $^{143}Nd/^{144}Nd$ value in CHUR is shown as a function of age in the neighborhood of 4.6 AE. If a solid object condensed from the solar nebula at 4.6 AE ago, it would have an initial $^{143}Nd/^{144}Nd$ ratio of 0.505829. Note the shift in $^{143}Nd/^{144}Nd$ for a change in choice of age.

T_C may represent ancient materials with a simple history. If $T_M^{Nd} > T_C$ or $T_M^{Nd} < T_C$, then this demonstrates open system behavior at times less than 4.6 AE. The model age T_M^{Nd} is a strict upper limit to the last time of disturbance of the system. As chemical fractionation for Sm relative to Nd is often small for total rocks, the T_M^{Nd} model ages are currently of far less utility than corresponding model ages for the Rb-Sr system where large chemical fractionations are common.

Model ages T_{CHUR}^{Nd} may be calculated relative to the CHUR curve [35,52,69] and corresponds to the time in the past at which the $^{143}Nd/^{144}Nd$ in the sample coincides with the $^{143}Nd/^{144}Nd$ in a chondritic reservoir:

$$T_{CHUR}^{Nd} = \frac{1}{\lambda} \ln\{1 + [(^{143}Nd/^{144}Nd)_{MEAS} - I_{CHUR}^{Nd}(0)] / [(^{147}Sm/^{144}Nd)_{MEAS} - (^{147}Sm/^{144}Nd)_{CHUR}^{0}]\} \quad (3)$$

This type of model age is equivalent to T_{ICE} ages of Lugmair et al. [58]. For typical continental crustal rocks which typically have Sm/Nd ratios that are 40% lower than the chondritic ratio, the new model parameters will only cause small changes in the previously published T_{CHUR}^{Nd} model ages. The T_{CHUR}^{Nd} age is exactly equal to the time when a magma is derived from the model CHUR reservoir *with* Sm/Nd fractionation. If the true parent reservoir is fractionated with regard to CHUR, then T_{CHUR}^{Nd} gives a time which in general is not related to a specific process either of magma generation or planetary differentiation.

8. Data representation

Papanastassiou and Wasserburg [41] first introduced an ϵ-notation for expressing the deviations of $^{87}Sr/^{86}Sr$ relative to a reference value. Following DePaolo and Wasserburg [34] the $^{143}Nd/^{144}Nd$ ratio in a reservoir j at time T is expressed as the fractional deviation in parts in 10^4 from that in CHUR at time T and denoted by $\epsilon_{Nd}^{j}(T)$. Let $I_j^{Nd}(T)$ be the $^{143}Nd/^{144}Nd$ ratio in a reservoir j at time T, then we have:

$$\epsilon_{Nd}^{j}(T) = 10^4\left[\frac{I_j^{Nd}(T)}{I_{CHUR}^{Nd}(T)} - 1\right] \quad (3)$$

A similar notation was also introduced independently by Lugmair et al. [58]. Here $I_{CHUR}^{Nd}(T)$ is given by equation (1) with j = CHUR. Initial $^{143}Nd/^{144}Nd$ ratios for a rock may be expressed in ϵ-units relative to the CHUR curve using equation (3). Then $I_j^{Nd}(T)$ is the initial value determined by an internal isochron or calculated from the present-day values of $^{143}Nd/^{144}Nd$ and $^{147}Sm/^{144}Nd$ of the rock and an independently determined age through equation (1). The measured present-day values of $^{143}Nd/^{144}Nd$ in rock samples relative to $I_{CHUR}^{Nd}(0)$ are also often given in ϵ-units and are denoted $\epsilon_{Nd}(0)$. We have chosen $I_{CHUR}^{Nd}(0) = 0.511836$ as before and a new value $(^{147}Sm/^{144}Nd)_{CHUR}^{0} = 0.1967$ which is 1.6% higher than the previous value of 0.1936 [58]. Values of $\epsilon_{Nd}(0)$ will be unchanged if they are referred to the above $I_{CHUR}^{Nd}(0)$ value. However, the $I_{CHUR}^{Nd}(T)$ values calculated from (1) will be changed and consequently $\epsilon_{Nd}(T)$ will also be changed due to the new value for $(^{147}Sm/^{144}Nd)_{CHUR}^{0}$. The $^{147}Sm/^{144}Nd$ ratio in a reservoir j is expressed as the enrichment factor relative to CHUR:

$$f_j^{Sm/Nd} = \frac{(^{147}Sm/^{144}Nd)_j}{(^{147}Sm/^{144}Nd)_{CHUR}^{0}} - 1 \quad (4)$$

and this value will also be changed. Model calculations for crust and mantle evolution can usually be made with linearized equations due to the long half-life of ^{147}Sm. Consider a reservoir j which is derived from CHUR in a single differentiation event at time T_D. As shown by DePaolo and Wasserburg [34], at a time T subsequent to the time of differentiation we have to a good approximation that:

$$\epsilon_{Nd}^{j}(T) = Q_{Nd} f_j^{Sm/Nd}(T_D - T) \quad (5)$$

where:

$$Q_{Nd} = 10^4\lambda(^{147}Sm/^{143}Nd)_{CHUR}^{0} \quad (6)$$

Similar equations have been shown by Jacobsen and Wasserburg [70] to be valid for models of continuous or multi-episodic evolution of crust and mantle, the only difference being the interpretation of the time parameter. The new values for CHUR give Q_{Nd} = 25.13 AE^{-1} (see Table 3) for $\lambda = 0.00654$ AE^{-1} as compared to the previous value of 24.73 AE^{-1}. These small changes will not cause any major revisions in previous model calculations. Although model calculation can be made with linearized equations such as

TABLE 3

Model parameters for CHUR

$$\left(\frac{^{143}\mathrm{Nd}}{^{144}\mathrm{Nd}}\right)^0_{\mathrm{CHUR}} = I^{\mathrm{Nd}}_{\mathrm{CHUR}}(0) = 0.511836$$

$$\left(\frac{^{147}\mathrm{Sm}}{^{144}\mathrm{Nd}}\right)^0_{\mathrm{CHUR}} = 0.1967$$

Initial ^{143}Nd/^{144}Nd at 4.60 AE: $I^{\mathrm{Nd}}_{\mathrm{CHUR}}(4.6\ \mathrm{AE}) = 0.505829$

$$Q_{\mathrm{Nd}} = 10^4\ \lambda \left(\frac{^{147}\mathrm{Sm}}{^{143}\mathrm{Nd}}\right)^0_{\mathrm{CHUR}} = 25.13 \times 10^{-9}\ \mathrm{yr}^{-1}$$

$\lambda = 6.54 \times 10^{-12}\ \mathrm{yr}^{-1}$

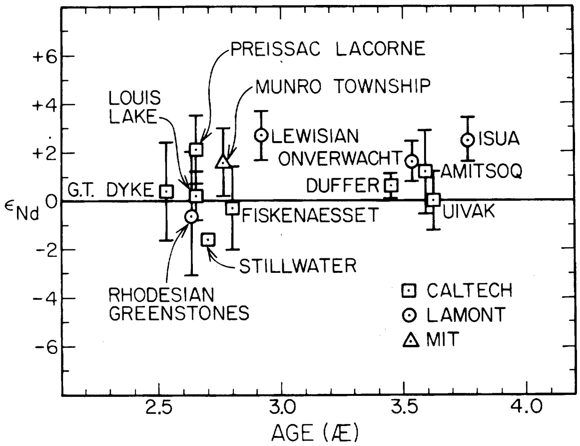

Fig. 7. Fractional deviations in parts in 10^4 of initial ^{143}Nd/^{144}Nd of Archean rocks, from evolution in the CHUR reservoir. Data for Stillwater, Great Dyke, Louis Lake batholith, Preissac Lacorne batholith, Fiskenaesset anorthosite, and Amitsoq gneiss from DePaolo and Wasserburg [34,52,71]; Duffer dacite and Uivak gneiss from McCulloch [35]; Rhodesian Greenstones, Lewisian granulite and amphibolite facies gneisses, Onverwacht volcanics, and Isua volcanics, from Hamilton et al. [62,72,73,74]. Note that there is only one data point with relatively small errors (Stillwater). More high-precision data are clearly needed.

(5), the calculation of initial ^{143}Nd/^{144}Nd values and the growth curves shown in Figs. 5 and 6 have to be calculated with the exact exponential form given in equation (1).

9. The Nd evolution curve for the earth

DePaolo and Wasserburg [34,52] discovered that for a wide variety of igneous rocks there were well defined values of the initial ^{143}Nd/^{144}Nd as a function of time (back to 3.6 AE ago) and that this appeared to represent the Nd evolution curve for the earth. They further showed that this curve was close to the average chondritic evolution as estimated from achondrite data (i.e., Juvinas). These general observations have been confirmed by several subsequent studies [35,62,71–75], although the fundamental question of which rocks are from pristine "primary" mantle sources has not yet been adequately resolved. The old CHUR curve was shown to be a reasonably good representation of the terrestrial values, although there are clear discrepancies for some young rocks and some precisely dated Archean rocks. We now want to address what the correlation looks like back through time using the new parameters. We therefore consider the data on Archean rocks where the claim has been made that most of the data fit the CHUR curve. All available Archean data for initial Nd are shown in Fig. 7 as deviations from the new CHUR curve. The small shifts in the CHUR evolution curve reported here do not alter the basic conclusions by other workers that the isotopic composition of Nd in a variety of crustal rocks approximates the evolution of a reservoir with chondritic Sm-Nd evolution. However, the more refined results reported here make it evident that more stringent tests are needed. Note that Fig. 7 combines data from three different laboratories, obtained both by direct total rock and/or mineral isochron determination and by indirect determination of initial Nd values using ages derived by other techniques. All techniques have some intrinsic problems. In addition, discrepancies in tracer calibrations and measurements of all Nd isotope ratios as discussed for the meteorite data may also exist for the terrestrial data. We have at present no direct way of evaluating how much of the variations shown in Fig. 7 could be due to such analytical difficulties. In the following discussion we will, however, *assume* that the deviations from the CHUR curve reflect real variations in initial ϵ_{Nd} values. Although the Archean data are furthest from the present-day data on which the CHUR curve is based, this portion of the CHUR curve is subject to rather small uncertainties as shown in Fig. 5 independent of the detailed choice of present-day reference value. If another chondritic value (±2 ϵ-units) which lies on the meteorite isochron shown in Fig. 2 were chosen to define the CHUR curve, it would not alter the conclusion for the Archean. It is clear that it is not possible to fit a single evolution curve through the data in Fig. 7 and the scatter of the data shows that deviations from the bulk earth curve must have occurred in the Archean. This scatter still exists regardless of the arbitrary choice of a reference curve. Assuming that the CHUR curve is representative of the bulk earth, it is clear that almost all data, except for the Stillwater results, plot on or above the new CHUR curve. The negative initial $\epsilon_{Nd} = -1.8 \pm 0.2$ at 2.7 AE ago of the Stillwater complex has been attributed as possibly being due to crustal contamination [71].

The data on the Lewisian rocks (2.9 AE) and the Isua volcanics (3.8 AE) now plot ~2.5 ϵ-units above the curve. These positive ϵ_{Nd} values indicate the presence of a depleted layer in the mantle throughout the Archean. Such a layer may represent the early evolution of the source of the present-day mid-ocean ridge basalts which today have $\epsilon_{Nd} \approx +10$. This implies that the source of the Isua volcanics was residual mantle material that was involved in crust-forming events at least 4.2 AE ago assuming $f^{Sm/Nd} = +0.22$ for the depleted mantle residue which was left after early continent formation [70]. Mantle-crust differentiation models in which melts that form new continental crust are formed from a mantle reservoir that is continuously depleted, such as Model II of Jacobsen and Wasserburg [70] and the bidirectional model of O'Nions et al. [76] cannot produce a value of $\epsilon_{Nd} = +2.5$ for the depleted mantle at 3.8 AE ago if the depleted mantle has $\epsilon_{Nd} = +10$ today. If the Isua ϵ_{Nd} value is characteristic of the depleted mantle 3.8 AE ago, then this is more consistent with a model where the mechanism for crustal growth is by deriving melts over the age of the earth by melting of undepleted mantle and the depleted residue is stored in a separate layer as in Model I of Jacobsen and Wasserburg [70].

Most of the other data shown in the figure are still within error of the CHUR curve; however, they are subject to rather large uncertainties. The only precise data point is for the Stillwater [71] which plots distinctly below the curve. The apparent deviations from the CHUR curve in this time region are rather large and comparable with the modern variations considering the shortened time scale. For a detailed understanding of the evolution of the Archean mantle, it will be necessary to obtain much more precise initial values and ages for Archean samples than are currently available.

The data summarized in this paper clearly show that the *average* present-day $^{143}Nd/^{144}Nd$ value of chondrites must be within 1–2 ϵ-units of the reference value we have chosen for CHUR and that the bulk earth value lies close to the chondritic value. We now wish to explore the implications of the case that the true bulk earth value is actually distinct from the $\epsilon_{Nd}^{CHUR}(T) \equiv 0$ curve within the limits given above. We currently would assign special significance to rocks that lie on the CHUR curve, namely, that they are derived from a reservoir which has not been subject to any substantial shift in the Sm/Nd ratio. This implies that this reservoir is either an undifferentiated primitive layer essentially unchanged since the formation of the earth or that this reservoir is a result of very early differentiation and contains essentially all of the incompatible elements as a result of a large degree of early partial melting. Both reservoirs would have the same isotopic characteristics with time but different bulk properties and concentrations of LIL elements. This class of magma reservoirs has been called primitive "unfractionated" or "undepleted". As shown schematically in Fig. 8, rocks (such as point $I_{CHUR}^{Nd}(0)$ or point V) whose initial values lie on this curve are then considered to be derived from such an "undepleted" source. Materials such as *DM* which today are far above the CHUR curve are taken to represent magmas derived from ancient depleted mantle, and material *CC* from far below the curve are taken to represent ancient enriched reservoirs (continental crust or remelted continental crust). Points A (and U) and B (and W) which are displaced somewhat above or below the CHUR curve are also taken to represent depleted or enriched mantle sources respectively, or blends with these characteristics. If the true bulk earth curve is represented by $I_{\oplus}^{Nd}(T)$ (see Fig. 8) and is distinct from $I_{CHUR}^{Nd}(T)$, then the extremely displaced points *DM* and *CC* still represent depleted and enriched reservoirs respectively, however, A, B, V, and W would then all represent enriched sources and U would represent a magma derived from

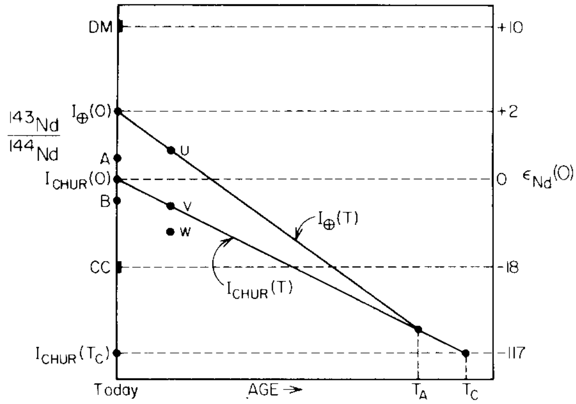

Fig. 8. Hypothetical evolution of $^{143}Nd/^{144}Nd$ for the earth (⊕) and CHUR. *DM* represents the average $\epsilon_{Nd}(0)$ value for depleted mantle as determined from mid-ocean ridge basalts, and *CC* the average $\epsilon_{Nd}(0)$ value for the continental crust. T_C is the time of condensation and T_A the time of accretion. The figure shows the hypothetical case where the bulk earth gets a 1.7% higher Sm/Nd ratio than that of CHUR during accretion. This results in an $\epsilon_{Nd}(0)$ value of +2 for the bulk earth today. As discussed in the text if this is the case then it may change our interpretation of data that follows the CHUR curve.

the undepleted reservoir. It follows that if the earth curve were displaced away from the CHUR curve by say $\epsilon_{Nd}^{\oplus}(0) = +2$, then many continental rocks (flood basalts, granites, etc.) would be inferred to come from enriched reservoirs. If the curve were displaced to say $\epsilon_{Nd}^{\oplus}(0) = -2$, then it would be interpreted as indicating their derivation from depleted sources. In any event, the attribution of a wide variety of crustal rock types as coming from an undepleted (≡ unfractionated relative abundances of LIL elements) mantle layer would be substantially changed. The existence of an unfractionated ancient mantle layer would thus be subject to serious revision (see schematic diagram of Fig. 8). The small magnitude of most Nd isotopic effects and the obviously complex nature of crustal and mantle evolution and crustal contamination problems may make the resolution of this issue difficult.

10. Lunar Nd evolution

In contrast to the earth, there is only a limited amount of knowledge of the temporal evolution of initial $^{143}Nd/^{144}Nd$ for the moon because of the limited range in ages of lunar rocks. In addition, if we assume that the lunar curve may be represented by the CHUR evolution curve, then it can be shown that many lunar rocks which crystallized 3–4 AE ago deviate greatly from the CHUR evolution line. The 3.2-AE-old Apollo 12 ilmenite basalts have $\epsilon_{Nd} \approx +12$ [45] which implies fractionations of up to 34% in the Sm/Nd ratio in the source reservoirs from which the lunar magmas were derived. In general the Sm-Nd isotopic data demonstrate that the mare basalts were derived from LREE-depleted sources which formed close to the origin of the moon and that the highland crust represents the complementary LREE-enriched material. This is true using both the old and the new CHUR evolution line. However, previous conclusions about early lunar differentiation from Sm-Nd model ages are very sensitive to small shifts in the model parameters [77]. Lugmair and coworkers [29,59], using the old CHUR curve (e.g., from Juvinas), suggested that Sm-Nd data on both mare basalts and highland samples require a time of early differentiation for the moon at 4.4 AE ago using T_{CHUR}^{Nd} model ages. In contrast mare basalts from this laboratory [49] and the data of Nyquist et al. [45] now have T_{CHUR}^{Nd} model ages of 5–6 AE and clearly do not precisely define the time of early differentiation of the moon as claimed by Lugmair. This is due to a decrease in the Sm/Nd ratio during basalt genesis as discussed in detail by Nyquist et al. [45]. The new CHUR values change the T_{CHUR}^{Nd} model ages for highland samples analyzed in this laboratory [35, 77] by about 0.5 AE to younger values (i.e., ~4.4 ± 0.2 AE) and are thus now in better agreement with Rb-Sr and U-Pb data on the same samples. However, the only precise age for early lunar differentiation is ~4.47 AE and comes from the upper intersection of the U-Pb cataclysm isochron [77]. The early attempts to calculate reliable T_{CHUR}^{Nd} ages are subject to large errors due to the small enrichment factors in most cases. These errors are in no way removed by the present revisions and considerable caution is still required in interpreting such ages as giving precise and reliable estimates of the times of early lunar differentiation. It is most likely that the young (4.2–4.3 AE) Rb-Sr model ages of highland rocks give a more reliable estimate of one of the times of the lunar differentiation [77] due to the much larger fractionations observed for the Rb-Sr system.

11. Conclusions

From the data presented we conclude that a self-consistent set of average present-day values for chondritic meteorites are $^{143}Nd/^{144}Nd = 0.511836$ and $^{147}Sm/^{144}Nd = 0.1967$. $^{143}Nd/^{144}Nd$ changes by 1 ϵ-unit in 39 m.y. in CHUR so the uncertainty in the *initial* time makes it difficult at present to know the initial solar value for $^{143}Nd/^{144}Nd$ precisely. These values are not consistent with most previously published achondrite data, but are consistent with our achondrite data and that reported by Nyquist et al. [45]. The presence of inter-laboratory discrepancies in meteorite data is evident and may be due to errors in Sm and Nd spike calibrations or to measurement of isotopic abundances. Some terrestrial Archean samples now show clear positive deviations from the CHUR evolution curve, which were not evident using the old model parameters for CHUR. The new parameters only make small changes in published T_{CHUR}^{Nd} model ages for highly fractionated samples.

Acknowledgements

This work has been supported by NSF grant EAR 76-22494 and NASA grant NGL 05-002-188. We thank D.A. Papanastassiou for his comments on the manuscript and his generous aid in matters spectrometric. We appreciate the thorough and scholarly reviews of the paper by L.E. Nyquist and N.M. Evensen which presumably led us to substantially improve the manuscript. The sources of the meteorite samples are as follows: Murchison, Field Museum of Natural History, Chicago. Juvinas and St. Severin, Museum of Natural History, Paris. Peace River, University of Alberta. Guareña, Museo Nacional de Ciencias Naturales de Madrid.

References

1 J.E. Ross and L.H. Aller, The chemical composition of the Sun, Science 191 (1976) 1223–1229.

2 V.M. Goldschmidt, Geochemische Verteilungsgesetze der Elemente, IX. Die Mengenverhältnisse der Elemente und der Atom-arten, Skr. Nor. Vidensk.-Akad. Oslo 1, 4 (1937) 1–148.

3 R.S. Maier and W. Whaling, Transition probabilities in Nd(II) and the solar neodymium abundance, J. Quant. Spectrosc. Radiat. Transfer 18 (1977) 501–507.

4 L. Saffman and W. Whaling, Transition probabilities in Sm(II) and the solar abundance of samarium, J. Quant. Spectrosc. Radiat. Transfer 21 (1979) 93–98.

5 H.Y. McSween, Are carbonaceous chondrites primitive or processed?, Rev. Geophys. Space Phys. 17 (1979) 1059–1078.

6 C.M. Gray, D.A. Papanastassiou and G.J. Wasserburg, The identification of early condensates from the solar nebula, Icarus 20 (1973) 213–239.

7 M.T. McCulloch and G.J. Wasserburg, Barium and neodymium isotopic anomalies in the Allende meteorite, Astrophys. J. 220 (1978) L15–L19.

8 M.T. McCulloch and G.J. Wasserburg, More anomalies from the Allende meteorite: samarium, Geophys. Res. Lett. 5 (1978) 599–602.

9 G.J. Wasserburg, D.A. Papanastassiou and H.G. Sanz, Initial strontium for a chondrite and the determination of a metamorphism or formation interval, Earth Planet. Sci. Lett. 7 (1969) 33–43.

10 G.J. Wasserburg, J.C. Huneke and D.S. Burnett, Correlation between fission tracks and fission type xenon in meteoritic whitlockite, J. Geophys. Res. 74 (1969) 4221–4232; Y. Cantelaube, M. Maurette and P. Pellas, Traces d'ions lourds dans les minéraux de la chondrite de Saint Séverin, in: Radioactive Dating and Methods of Low-level Counting (International Atomic Energy Agency, Vienna, 1967) 215–229.

11 G. Manhes, J.F. Minster and C.J. Allègre, Comparative uranium-thorium-lead and rubidium-strontium study of the Saint Séverin amphoterite: consequences for early solar system chronology, Earth Planet. Sci. Lett. 39 (1978) 14–24.

12 R.S. Lewis, Rare gases in separated whitlockite from St. Severin chondrite: xenon and krypton from fission of extinct ^{244}Pu, Geochim. Cosmochim. Acta 39 (1975) 417–432.

13 J.H. Jones and D.S. Burnett, The distribution of U and Pu in the St. Severin chondrite, Geochim. Cosmochim. Acta 43 (1979) 1895–1905.

14 G.W. Lugmair, Sm-Nd ages: a new dating method, Meteoritics 9 (1974) 369 (abstract).

15 S.B. Jacobsen and G.J. Wasserburg, Sm-Nd isotopic systematics of chondrites, in: Lunar and Planetary Science XI (The Lunar and Planetary Institute, Houston, Texas, 1980) 502–504 (abstract).

16 S.B. Jacobsen, Study of crust and mantle differentiation processes from variations in Nd, Sr, and Pb isotopes, Ph.D. Thesis, California Institute of Technology, Pasadena, Calif. (1980).

17 L.A. Haskin and M.A. Gehl, The rare-earth distribution in sediments, J. Geophys. Res. 67 (1962) 2537–2541.

18 R.A. Schmitt, R.H. Smith, J.E. Lasch, A.W. Mosen, D.A. Olehy and J. Vasilevskis, Abundances of fourteen rare-earth elements, scandium and yttrium in meteoritic

and terrestrial matter, Geochim. Cosmochim. Acta 27 (1963) 577–622.
19 R.A. Schmitt, R.H. Smith and D.A. Olehy, Rare earth, yttrium and scandium abundances in meteoritic and terrestrial matter, II, Geochim. Cosmochim. Acta 28 (1964) 67–86.
20 P.W. Gast, N.J. Hubbard and H. Weismann, Chemical composition and petrogenesis of basalts from Tranquillity Base, Proc. Apollo 11 Lunar Sci. Conf. (1970) 1143–1163.
21 C.C. Schnetzler and M.L. Bottino, Some alkali, alkaline-earth and rare earth element concentrations and the Rb-Sr age of the Lost City meteorite and separated phases, J. Geophys. Res. 76 (1971) 4061–4066.
22 A. Masuda, N. Nakamura and T. Tanaka, Fine structures of mutually normalized rare-earth patterns of chondrites, Geochim. Cosmochim. Acta 37 (1973) 239–248.
23 N. Nakamura and A. Masuda, Chondrites with peculiar rare-earth patterns, Earth Planet. Sci. Lett. 19 (1973) 429–437.
24 N. Nakamura, Determination of REE, Ba, Fe, Mg, Na, and K in carbonaceous and ordinary chondrites, Geochim. Cosmochim. Acta 38 (1974) 757–775.
25 N.M. Evensen, P.J. Hamilton and R.K. O'Nions, Rare-earth abundances in chondritic meteorites, Geochim. Cosmochim. Acta 42 (1978) 1199–1212.
26 T. Tanaka and A. Masuda, Rare-earth elements in matrix, inclusions and chondrules of the Allende meteorite, Icarus 19 (1973) 523–530.
27 K. Notsu and H. Mabuchi, The samarium-neodymium chronology of chondrites, Geochem. J. 9 (1975) 97–106.
28 G.W. Lugmair, N.B. Scheinin and K. Marti, Search for extinct ^{146}Sm, 1. The isotopic abundance of ^{142}Nd in the Juvinas meteorite, Earth Planet. Sci. Lett. 27 (1975) 79–84.
29 G.W. Lugmair, N.B. Scheinin and K. Marti, Sm-Nd age and history of Apollo 17 basalt 75075: evidence for early differentiation of the Lunar exterior, Proc. 6th Lunar Planet. Sci. Conf. (1975) 1419–1429.
30 C.J. Allègre, J.L. Birck, S. Fourcade and M. Semet, ^{87}Rb/^{87}Sr age of the Juvinas basaltic achondrite and early igneous activity of the solar system, Science 187 (1975) 436–438.
31 J.W. Larimer, The condensation and fractionation of refractory lithophile elements, Icarus 40 (1979) 446–454.
32 W.V. Boynton, Fractionation in the solar nebula: condensation of yttrium and the rare earth elements, Geochim. Cosmochim. Acta 39 (1975) 569–584.
33 W.V. Boynton, R.M. Frazier and J.D. Macdougall, Identification of an ultra-refractory component in the Murchison meteorite, in: Lunar and Planetary Science XI (The Lunar and Planetary Institute, Houston, Texas, 1980) 103–105 (abstract).
34 D.J. DePaolo and G.J. Wasserburg, Nd isotopic variations and petrogenetic models, Geophys. Res. Letts. 3 (1976) 249–252.
35 M.T. McCulloch, Part I: Sm-Nd and Rb-Sr chronology of crustal formation. Part II: Ba, Nd, and Sm isotopic anomalies in the Allende meteorite, Ph.D. Thesis, California Institute of Technology, Pasadena, Calif. (1979).
36 C.C. Patterson, H. Brown, G.R. Tilton and M. Inghram, Concentration of uranium and lead and the isotopic composition of lead in meteoritic material, Phys. Rev. 92 (1953) 1234–1235.
37 M. Tatsumoto, R.J. Knight and C.J. Allègre, Time differences in the formation of meteorites as determined from the ratio of lead-207 to lead-206, Science 180 (1973) 1279–1283.
38 J.M. Huey and T.P. Kohman, ^{207}Pb-^{206}Pb isochron and age of chondrites, J. Geophys. Res. 78 (1973) 3227–3244.
39 G.R. Tilton, Isotopic lead ages of chondritic meteorites, Earth Planet. Sci. Lett. 19 (1973) 321–329.
40 M. Tatsumoto, D.M. Unruh and G.A. Desborough, U-Th-Pb and Rb-Sr systematics of Allende and U-Th-Pb systematics of Orgueil, Geochim. Cosmochim. Acta 40 (1976) 617–634.
41 D.A. Papanastassiou and G.J. Wasserburg, Initial strontium isotopic abundances and the resolution of small time differences in the formation of planetary objects, Earth Planet. Sci. Lett. 5 (1969) 361–376.
42 G.J. Wasserburg, F. Tera, D.A. Papanastassiou and J.C. Huneke, Isotopic and chemical investigations on Angra dos Reis, Earth Planet. Sci. Lett. 35 (1977) 294–316.
43 P.W. Gast, The isotopic composition of strontium and the age of stone meteorites, I, Geochim. Cosmochim. Acta 26 (1962) 927–943.
44 J.L. Birck and C.J. Allègre, Chronology and chemical history of the parent body of basaltic acondrites studied by the ^{87}Rb-^{87}Sr method, Earth Planet. Sci. Lett. 39 (1978) 37–51.
45 L.E. Nyquist, C.-Y. Shih, J.L. Wooden, B.M. Bansal and H. Wiesmann, The Sr and Nd isotopic record of Apollo 12 basalts: implications for lunar geochemical evolution, Proc. 10th Lunar Planet. Sci. Conf. (1979) 77–114.
46 O. Hauge. A search for the solar ^{87}Sr content and the solar Rb/Sr ratio, Solar Phys. 26 (1972) 276–282.
47 O. Eugster, F. Tera, D.S. Burnett and G.J. Wasserburg, Isotopic composition of Gadolinium and neutron capture effects in some meteorites, J. Geophys. Res. 75 (1970) 2753–2768.
48 G.J. Wasserburg, D.A. Papanastassiou, E.V. Nenow and C.A. Bauman, A programmable magnetic field mass spectrometer with on-line data processing, Rev. Sci. Instrum. 40 (1969) 288–295.
49 D.A. Papanastassiou, D.J. DePaolo and G.J. Wasserburg, Rb-Sr and Sm-Nd chronology and genealogy of basalts from the Sea of Tranquillity, Proc. 8th Lunar Planet. Sci. Conf. (1977) 1639–1672.
50 D.J. DePaolo, Study of magma sources, mantle structure and the differentiation of the earth from variations of ^{143}Nd/^{144}Nd in igneous rocks, Ph.D. Thesis, California Institute of Technology, Pasadena, Calif. (1978).

51 A.O. Nier, A redetermination of the relative abundances of the isotopes of carbon, nitrogen, oxygen, argon, and potassium, Phys. Rev. 77 (1950) 789–793.
52 D.J. DePaolo and G.J. Wasserburg, Inferences about magma sources and mantle structure from variations of $^{143}Nd/^{144}Nd$, Geophys. Res. Lett. 3 (1976) 743–746.
53 G.P. Russ, III, Neutron stratigraphy in the lunar regolith, Ph.D. Thesis, California Institute of Technology, Pasadena, Calif. (1974).
54 G.P. Russ, D.S. Burnett, R.E. Lingenfelter and G.J. Wasserburg, Neutron capture on ^{149}Sm in lunar samples, Earth Planet. Sci. Lett. 13 (1971) 53–60.
55 G.W. Lugmair and K. Marti, Sm-Nd-Pu timepieces in the Angra dos Reis meteorite, Earth Planet. Sci. Lett. 35 (1977) 273–284.
56 J. Hamet, N. Nakamura, D.M. Unruh and M. Tatsumoto, Origin and history of the adcumulate eucrite, Moama as inferred from REE abundances, Sm-Nd and U-Pb systematics, Proc. 9th Lunar Planet. Sci. Conf. (1978) 1115–1136.
57 K. Notsu, H. Mabuchi, O. Yoshioka, J. Matsuda and M.Ozima, Evidence of the extinct nuclide ^{146}Sm in "Juvinas" achondrite, Earth Planet. Sci. Lett. 19 (1973) 29–36.
58 G.W. Lugmair, K. Marti, J.P. Kurtz and N.B. Scheinin, History and genesis of lunar troctolite 76535 or: How old is old?, Proc. 7th Lunar Planet. Sci. Conf. (1976) 2009–2033.
59 G.W. Lugmair and R.W. Carlson, The Sm-Nd history of KREEP, Proc. 9th Lunar Planet. Sci. Conf. (1978) 689–704.
60 N. Nakamura, M. Tatsumoto, P.D. Nunes, D.M. Unruh, A.P. Schwab, and T.R. Wildeman, 4.4 b.y.-old clast in Boulder 7, Apollo 17: a comprehensive chronological study by U-Pb, Rb-Sr, and Sm-Nd methods, Proc. 7th Lunar Planet. Sci. Conf. (1976) 2309–2333.
61 D.M. Unruh, N. Nakamura and M. Tatsumoto, History of the Pasamonte achondrite: relative susceptibility of the Sm-Nd, Rb-Sr, and U-Pb systems to metamorphic events, Earth Planet. Sci. Lett. 37 (1977) 1–12.
62 P.J. Hamilton, R.K. O'Nions, N.M. Evensen, D. Bridgwater and J. Allaart, Sm-Nd isotopic investigations of the Isua supracrustals, West Greenland: implications for mantle evolution, Nature 272 (1978) 41–43.
63 T. Lee, D.A. Papanastassiou and G.J. Wasserburg, Demonstration of ^{26}Mg excess in Allende and evidence for ^{26}Al, Geophys. Res. Lett. 3 (1976) 109–112.
64 T. Lee, D.A. Papanastassiou and G.J. Wasserburg, ^{26}Al in the early solar system: fossil or fuel?, Astrophys. J. 211 (1977) L107–L110.
65 V.S. Safranov, Evolution of the Protoplanetary Cloud and the Formation of the Earth and Planets (Nauka Moscow) (in Russian). English transl. as NASA TT F-677, NTIS, Springfield, Va. (1972).
66 F. Tera and G.J. Wasserburg, U-Th-Pb systematics on lunar rocks and inferences about lunar evolution and the age of the moon, Proc. 5th Lunar Planet. Sci. Conf. (1974) 1571–1599.
67 A.J. Gancarz and G.J. Wasserburg, Initial Pb of the Amitsoq gneiss, west Greenland, and implications for the age of the earth, Geochim. Cosmochim. Acta 41 (1977) 1283–1301.
68 G.J. Wasserburg and D.A. Papanastassiou, Model ages, Nature 259 (1976) 159–160.
69 M.T. McCulloch and G.J. Wasserburg, Sm-Nd and Rb-Sr chronology of continental crust formation, Science 200 (1978) 1003–1011.
70 S.B. Jacobsen and G.J. Wasserburg, The mean age of mantle and crustal reservoirs, J. Geophys. Res. 84 (1979) 7411–7427.
71 D.J. DePaolo and G.J. Wasserburg, Sm-Nd age of the Stillwater Complex and the mantle evolution curve for neodynium, Geochim. Cosmochim. Acta 43 (1979) 999–1008.
72 P.J. Hamilton, R.K. O'Nions and N.M. Evensen, Sm-Nd dating of Archean basic and ultrabasic volcanics, Earth Planet. Sci. Lett. 36 (1977) 263–268.
73 P.J. Hamilton, N.M. Evensen, R.K. O'Nions and J. Tarney, Sm-Nd systematics of Lewisian gneisses: implications for the origin of granulites, Nature 277 (1979) 25–28.
74 P.J. Hamilton, N.M. Evensen, R.K. O'Nions, H.S. Smith and A.J. Erlank, Sm-Nd dating of Onverwacht Group Volcanics, southern Africa, Nature 279 (1979) 298–300.
75 A. Zindler, C. Brooks, N.T. Arndt and S. Hart, Nd and Sr isotope data from komatiitic and tholeiitic rocks of Munro Township, Ontario, in: Short Papers of the 4th Int. Conf. Geochronology, Cosmochronology and Isotope Geology, U.S. Geol. Surv., Open-File Rep. 78-701 (1978) 469–471.
76 R.K. O'Nions, N.M. Evensen and P.J. Hamilton, Geochemical modeling of mantle differentiation and crustal growth, J. Geophys. Res. 84 (1979) 6091–6101.
77 F. Oberli, M.T. McCulloch, F. Tera, D.A. Papanastassiou and G.J. Wasserburg, Early lunar differentiation constraints from U-Th-Pb, Sm-Nd, and Rb-Sr model ages, in: Lunar and Planetary Science IX (The Lunar and Planetary Institute, Houston, Texas, 1978) 832–834 (abstract).